

# Analysis of resonant inelastic x-ray scattering in $\text{La}_2\text{CuO}_4$

Takuji Nomura\*

*Synchrotron Radiation Research Center, Japan Atomic Energy Research Institute, Hyogo 679-5148, Japan*

Jun-ichi Igarashi

*Department of Mathematical Sciences, Ibaraki University, Ibaraki 310-8512, Japan*

(Dated: October 31, 2018)

We provide a semiquantitative explanation of a recent experiment on the resonant inelastic x-ray scattering (RIXS) in insulating cuprate  $\text{La}_2\text{CuO}_4$  (Y.J. Kim et al., Phys. Rev. Lett. **89**, 177003 (2002)). We show theoretically that there are three characteristic peaks in RIXS spectra, two of which are attributed to the charge transfer excitation and are reasonably assigned to those observed experimentally. The lowest energy peak has a relatively large dispersion ( $\sim 0.8$  eV) and is suppressed near the zone corner  $(\pi, \pi)$ , in agreement with the experiment. We stress that electron correlation is an essential factor for explaining the overall energy-momentum dependence of the RIXS spectra consistently.

PACS numbers: 78.70.Ck, 74.72.Dn, 78.20.Bh

## I. INTRODUCTION

Recently it has been revealed that resonant inelastic x-ray scattering (RIXS) is a powerful tool for elucidating the electronic properties of solids<sup>1</sup>. RIXS is a unique technique of detecting the relatively high-energy (of the order of 1 eV) charge excitations in solids. It is naturally expected that excitation spectra in such a high-energy regime reflect not only detailed electronic structures over a wide energy range but also electron correlations originating from strong electron-electron Coulomb repulsion. However, unfortunately, there are still only a few theoretical works on analyzing the effects of electron correlations on such high-energy excitation properties.

RIXS measurement in the hard x-ray regime has been applied to search for charge excitation modes and to determine the momentum dependence of charge excitation in several transition metal oxides, with the incident photon energy tuned to the absorption  $K$  edge<sup>2,3,4,5,6</sup>. A number of insulating cuprates have been investigated up to now, under the expectation that such a kind of excitations might be related to the unconventional high- $T_c$  superconductivity. For example, Kim et al. recently reported a detailed study of the momentum dependence of the charge transfer (CT) excitation spectra in  $\text{La}_2\text{CuO}_4$  (Fig. 1)<sup>5</sup>. They observed two characteristic peaks in the spectra at around  $\omega \sim 2.2$  eV and  $\sim 3.9$  eV at the zone center, by setting the incident photon energy to the Cu absorption  $K$  edge. The low-energy peak at 2.2 eV shifts to  $\omega \sim 3$  eV around  $(\pi, 0)$ , and becomes very small around the zone corner  $(\pi, \pi)$ . They considered that the two peaks with such a highly dispersive behavior are attributable to some kind of bound excitons which are formed as a result of Coulomb interaction, since such a bound exciton could move without disturbing the antiferromagnetically ordered background.

In this article, we provide an explanation of the RIXS spectra for the typical antiferromagnetic charge transfer insulator  $\text{La}_2\text{CuO}_4$  at a microscopic scale, by calculating

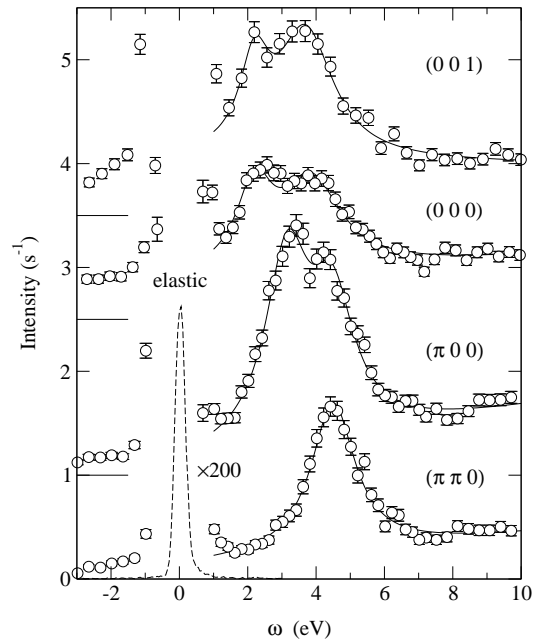


FIG. 1: RIXS spectra obtained by Kim et al. are shown for various momentum transfers as a function of energy transfer. (Reproduced from Ref. 5.)

the transition probability in the RIXS process. In order to investigate electron correlation effects in the RIXS process, we use the perturbative method developed by Platzman and Isaacs<sup>7</sup>. The scattering probability is calculated in the manner adopted by Nozières and Abrahams to discuss Fermi edge singularity in metals<sup>8</sup>. We use the Hartree-Fock (HF) theory to describe the antiferromagnetic ground state, and take account of the electron correlations in the scattering process within the random phase approximation (RPA). The perturbative method for band models compares well with other theoretical techniques based on a local atomic picture, such as exact diagonalization for a small cluster<sup>9</sup>. We obtain

a three-peak structure in the spectra at around 2, 5 and 9 eV, by taking account of the O2*p* band explicitly. The spectrum obtained as a function of energy loss shows dispersive behavior depending on the momentum transfer. In particular, the lowest energy spectral weight around 2 eV shows a relatively large dispersion ( $\sim 0.8$  eV), and becomes small around  $(\pi, \pi)$ , in agreement with the experiment. The two peaks at around 2 and 5 eV correspond to charge transfer excitations and are assigned to those observed in the experiment by Kim et al.<sup>5</sup>.

## II. MODEL AND THEORY

We introduce the model Hamiltonian for the system in the form  $H = H_{dp} + H_{1s-3d} + H_{1s} + H_{4p} + H_x$ .  $H_{dp}$ ,  $H_{1s}$

$$H_{dp} = \sum_{\mathbf{k}\sigma} \epsilon_d d_{\mathbf{k}\sigma}^\dagger d_{\mathbf{k}\sigma} + \sum_{\mathbf{k}\ell\ell'\sigma} \zeta_{p_\ell p_{\ell'}}(\mathbf{k}) p_{\mathbf{k}\ell\sigma}^\dagger p_{\mathbf{k}\ell'\sigma} + \sum_{\mathbf{k}\ell\sigma} (\xi_{dp_\ell}(\mathbf{k}) d_{\mathbf{k}\sigma}^\dagger p_{\mathbf{k}\ell\sigma} + \text{h.c.}) + \frac{U_{dd}}{N} \sum_{\mathbf{k}\mathbf{k}'\mathbf{q}} d_{\mathbf{k}'+\mathbf{q}\uparrow}^\dagger d_{\mathbf{k}-\mathbf{q}\downarrow}^\dagger d_{\mathbf{k}\downarrow} d_{\mathbf{k}'\uparrow}, \quad (1)$$

where  $d_{\mathbf{k}\sigma}$  and  $p_{\mathbf{k}\ell\sigma}$  ( $d_{\mathbf{k}\sigma}^\dagger$  and  $p_{\mathbf{k}\ell\sigma}^\dagger$ ) are annihilation (creation) operators for Cu3*d*<sub>*x*<sup>2</sup>-*y*<sup>2</sup></sub> and O2*p*<sub>*l*</sub> electrons ( $l = x, y$ ) with momentum  $\mathbf{k}$  and spin  $\sigma$ , respectively. We adopt the dispersion relations  $\xi_{dp_\ell}(\mathbf{k}) = 2it_{dp} \sin \frac{k_\ell}{2}$ ,  $\zeta_{p_\ell p_\ell}(\mathbf{k}) = \epsilon_p = 0$ , and  $\zeta_{p_x p_y}(\mathbf{k}) = \zeta_{p_y p_x}(\mathbf{k}) = 4t_{pp} \sin \frac{k_x}{2} \sin \frac{k_y}{2}$ , where  $t_{dp} = 1.3$  eV and  $t_{pp} = 0.65$  eV, which were estimated from LDA calculations<sup>10</sup>. The Coulomb energy and the charge transfer energy in HF theory are  $U_{dd} = 11$  eV and  $\epsilon_d^{HF} = -0.7$  eV, respectively. Within HF theory, we obtain the antiferromagnetic ground state with staggered spin moment  $m = 0.46\mu_B$  for the present parameter set.  $H_{1s-3d}$  gives the interaction between Cu1*s* holes and Cu3*d* electrons:

$$H_{1s-3d} = \frac{V}{N} \sum_{\mathbf{k}\mathbf{k}'\mathbf{q}\sigma\sigma'} d_{\mathbf{k}'+\mathbf{q}\sigma}^\dagger s_{\mathbf{k}-\mathbf{q}\sigma'}^\dagger s_{\mathbf{k}\sigma'} d_{\mathbf{k}'\sigma}, \quad (2)$$

where  $V$  is the core hole potential and is taken to be 15 eV, and  $s_{\mathbf{k}\sigma}$  ( $s_{\mathbf{k}\sigma}^\dagger$ ) is the annihilation (creation) operator for Cu1*s* electrons with momentum  $\mathbf{k}$  and spin  $\sigma$ .  $H_x$  describes the transitions between the Cu1*s* and Cu4*p* states, which involve photon absorption and inverse emission processes.  $H_x$  is of the form

$$H_x = \sum_{\mathbf{k}\mathbf{q}\sigma} (w(\mathbf{q}; \mathbf{k}) p_{\mathbf{k}+\mathbf{q}\sigma}^\dagger s_{\mathbf{k}\sigma} + \text{h.c.}), \quad (3)$$

where  $p^\dagger$  is the creation operator of the Cu4*p* electron. Since the Cu1*s* wave function is highly localized in the coordinate space, the wave functions of the Cu4*p* band states only in the region close to the origin contribute to

and  $H_{4p}$  describe the kinetics of Cu3*d*<sub>*x*<sup>2</sup>-*y*<sup>2</sup></sub> (hybridized with O2*p* orbitals), Cu1*s* and Cu4*p* electrons, respectively. We take a completely flat band for the Cu1*s* electron, which is well localized in the solid. In addition, for the Cu4*p* electrons, we take a simple cosine-shaped band with the energy minimum at the zone center. In any case, no detailed structure of the Cu4*p* band is required to determine the shape of RIXS spectra, since the factor including the dispersion function of the Cu4*p* band is integrated up with respect to the momentum and does not affect the momentum-energy dependence of the spectra, as we see later. For  $H_{dp}$ , we use a two-dimensional *dp*-model:

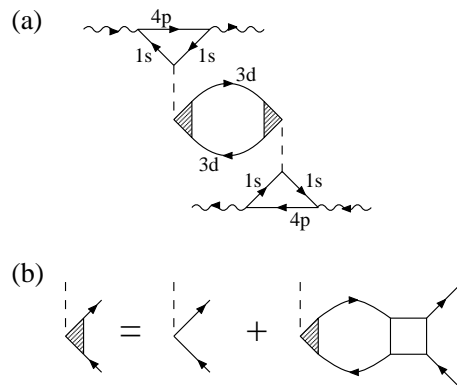


FIG. 2: (a) Diagram for the transition probability in the RIXS process. Green's functions for Cu1*s*, 4*p* and 3*d* electrons are assigned to the solid lines with '1*s*', '4*p*' and '3*d*', respectively. The wavy and broken lines represent the photon propagator and core hole potential  $V$ , respectively. The shaded triangle is the effective scattering vertex renormalized by Coulomb interaction  $U_{dd}$ . (b) Vertex renormalization in RPA. The empty square represents antisymmetrized bare Coulomb interaction between Cu3*d* electrons.

the matrix elements. This strong local nature results in the momentum independence of the matrix elements. In the present article, we ignore the momentum dependence of the matrix elements  $w(\mathbf{q}; \mathbf{k})$ , i.e.,  $w(\mathbf{q}; \mathbf{k}) = w$ .

In the RIXS process in La<sub>2</sub>CuO<sub>4</sub>, the following scattering channel is expected to predominantly contribute to the main spectral weight: the incident x-ray with the

1s-4p absorption energy excites the Cu1s electron to the Cu4p state. In the intermediate state, the created Cu1s core hole plays the role of a localized strong scattering body for the Cu3d electrons near the chemical potential. After the core hole scatters the Cu3d electron system from the ground state to some excited states (the most probable scattering process is the creation of only one electron-hole pair), the core hole is annihilated together with the Cu4p electron and a photon is emitted in the final state. Compared with the incident absorbed photon, the emitted photon loses momentum and energy

in amounts equal to those transferred to the Cu3d-O2p electrons. In the final state, after the Cu1s core hole disappears, an electron-hole pair remains on the Cu3d-O2p band. In the present study, we consider the lowest order in the core hole potential  $V$ , i.e., simple Born scattering of Cu3d electrons by the core hole. The transition probability for the total process is diagrammatically expressed in Fig. 2(a). The diagram in Fig. 2(a) is converted straightforwardly to an analytic expression in the same way as described in Ref. 8:

$$W(q_i, q_f) = (2\pi)^3 N |w|^4 \sum_{\mathbf{k}j j'} \delta(E_j(\mathbf{k}) + \omega - E_{j'}(\mathbf{k} + \mathbf{q})) n_j(\mathbf{k})(1 - n_{j'}(\mathbf{k} + \mathbf{q})) \times \left| \sum_{\sigma\sigma'} U_{j,d\sigma}(\mathbf{k}) \Lambda_{\sigma\sigma'}(\omega, \mathbf{q}) U_{d\sigma',j'}^\dagger(\mathbf{k} + \mathbf{q}) \sum_{\mathbf{k}_1} \frac{V}{(\omega_i + \epsilon_{1s} + i\Gamma_{1s} - \epsilon_{4p}(\mathbf{k}_1))(\omega_f + \epsilon_{1s} + i\Gamma_{1s} - \epsilon_{4p}(\mathbf{k}_1))} \right|^2, \quad (4)$$

where  $j^{(i)}$  characterizes the diagonalized band,  $E_j(\mathbf{k})$  is the energy dispersion of the band  $j$ ,  $q_i = (\omega_i, \mathbf{q}_i)$  [ $q_f = (\omega_f, \mathbf{q}_f)$ ] is the energy-momentum of the initially absorbed [finally emitted] photon, and the energy and momentum transfers are given by  $\omega = \omega_i - \omega_f$  and  $\mathbf{q} = \mathbf{q}_i - \mathbf{q}_f$ .  $\epsilon_{1s}$  and  $\epsilon_{4p}(\mathbf{k}_1)$  are the kinetic energies of the Cu1s and Cu4p electrons, respectively.  $n_j(\mathbf{k})$  is the electron occupation number at momentum  $\mathbf{k}$  in energy band  $j$ .  $U_{j,d\sigma}(\mathbf{k})$  is the  $(j, d\sigma)$ -element of the diagonalization matrix of the HF Hamiltonian. We set the incident photon energy near the absorption edge, i.e.,  $\omega_i \approx \epsilon_{4p}(0) - \epsilon_{1s}$ , and assume that the decay rate of the Cu1s hole is  $\Gamma_{1s} = 0.8$  eV. In the present study, we simply use the vertex function  $\Lambda_{\sigma\sigma'}(q)$  within RPA. The vertex renormalization within RPA is diagrammatically represented in Fig. 2(b). It is interesting to note that the factor  $n_j(\mathbf{k})|U_{j,d\sigma}(\mathbf{k})|^2 [(1 - n_{j'}(\mathbf{k} + \mathbf{q}))|U_{d\sigma',j'}^\dagger(\mathbf{k} + \mathbf{q})|^2]$  in Eq. (4) represents the partial occupation number of the Cu3d electron [hole] with momentum  $\mathbf{k}$  [ $\mathbf{k} + \mathbf{q}$ ] and spin  $\sigma$  [ $\sigma'$ ] in the band  $j$  [ $j'$ ]. According to our investigations, the product  $n_j(\mathbf{k})(1 - n_{j'}(\mathbf{k} + \mathbf{q}))|U_{j,d\sigma}(\mathbf{k})U_{d\sigma',j'}^\dagger(\mathbf{k} + \mathbf{q})|^2$  is the dominant factor in the scattering amplitude. Therefore, the RIXS spectrum in  $\text{La}_2\text{CuO}_4$  reflects the Cu3d partial electron and hole occupation numbers, that is, the Cu3d partial density of states.

### III. RESULTS

The numerical results of the RIXS intensity calculated using Eq. (4) are displayed in Fig. 3. We see the three characteristic peaks at around  $\omega \sim 2, 5$  and 9 eV. The lowest energy peak at 2 eV shows relatively large dispersive behavior. The peak shifts by approximately 0.8 eV

at  $\mathbf{q} \approx (\pi, 0)$  and becomes small at  $\mathbf{q} \approx (\pi, \pi)$ . This characteristic momentum dependence is consistent with the results in Fig. 1. The peak at 5 eV is assigned to the peak observed experimentally at 3.9 eV. The crude tight-binding fitting would be responsible for the 1 eV deviation of the peak position, and would still be insufficient to reproduce the electronic structure in such a high-energy region. The two peaks at 2 and 5 eV originate from CT excitation: Cu3d electrons hybridized with the O2p band are excited to the upper Cu3d band. This two-peak structure is a result of the structure of the Cu3d partial density of states mixed in the broad O2p band. On the other hand, the small peak at around 9 eV corresponds to the transition from the Cu3d lower Hubbard band to the Cu3d upper Hubbard band. The transition probability for this 9 eV process is relatively low. This is because the majority spin state at a local Cu site is almost fully occupied by one electron, and the hole occupation number in that state is almost zero. The actual localized moment will be almost  $1\mu_B$ , since the electron occupation number per one Cu site is almost one. As we have mentioned above, the intensity is closely related to the product of the Cu3d electron occupation number and the Cu3d hole occupation number. In the local picture, this product is expressed as  $n_{d,i\sigma}(1 - n_{d,i\sigma})$  ( $n_{d,i\sigma}$  is Cu3d electron number at Cu site  $i$  with spin  $\sigma$ ), and becomes almost zero in the limit of  $m = 1\mu_B$ . In the present HF calculation, we may have underestimated the electron occupation number in the majority spin state at a Cu site. In other words the magnetic moment  $m = 0.46\mu_B$  obtained in the HF theory might be smaller than the actual localized moment. Therefore, we should consider that the present method still overestimates the transition probability for this 9 eV process. Actually, the intensity for this process would be too small to be observed. Therefore this 9 eV

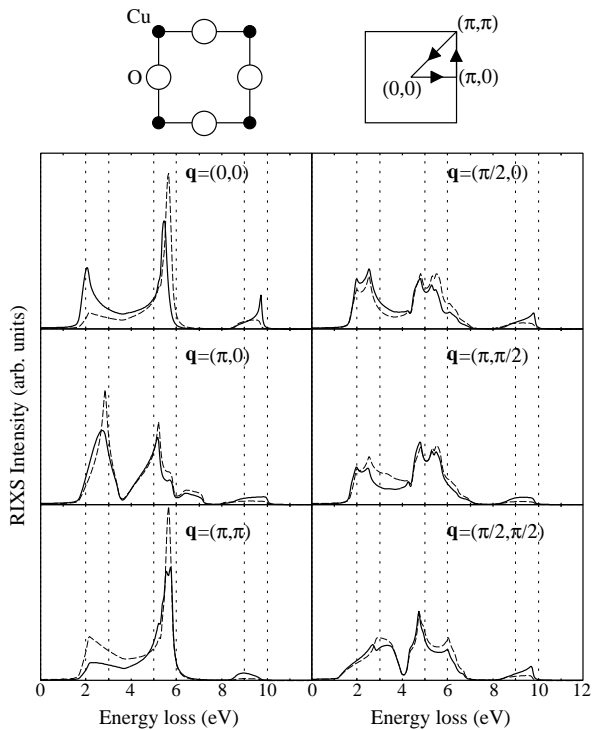


FIG. 3: The upper figures show the Cu-O plaquette and the contour in the first Brillouin zone (BZ). The lower six panels show the RIXS spectra as a function of the energy loss  $\omega = \omega_i - \omega_f$  on the above contour in BZ. The thick solid (thin broken) curves are results obtained with (without) RPA vertex renormalization.

weight should not be identified with the 7.2 eV peak observed in the experiment (peak c in Ref. 5), whose origin should be discussed on the basis of other scenarios.

Here we inspect the electronic structure and the density of states (DOS) of the model in the antiferromagnetic ground state. The Cu3d partial density of states (PDOS) and the total density of states are displayed in Fig. 4. The 2 and 5 eV RIXS peaks are assigned to the electronic excitation processes from the Cu3d PDOS weights around  $\omega \approx -1$  and  $-4$  (eV) to the upper Cu3d band around  $\omega \approx 2$  (eV), respectively. These Cu3d PDOS weights around  $\omega \approx -1$  and  $-4$  (eV) originate from the strong hybridization of the Cu3d and O2p orbitals. Therefore the two peak structures are attributed to Cu3d-O2p CT excitations.

It is of interest to discuss the effect of the correlations on the shape of the spectra. In Fig. 3, we compare the RPA-corrected case with the uncorrected case (i.e., zero order in  $U_{dd}$ :  $\Lambda_{\sigma\sigma'}(q) \rightarrow \delta_{\sigma\sigma'}$  in Eq. (4)). We find that the lowest order uncorrected calculation reproduces roughly the overall structure of the RIXS spectra. This is because the spectral weight is determined mainly by the partial occupation number of Cu3d electrons in each band, and the detailed scattering process is not necessary in the first step of analysis. However, the low energy peak structure at around 2 eV is modi-

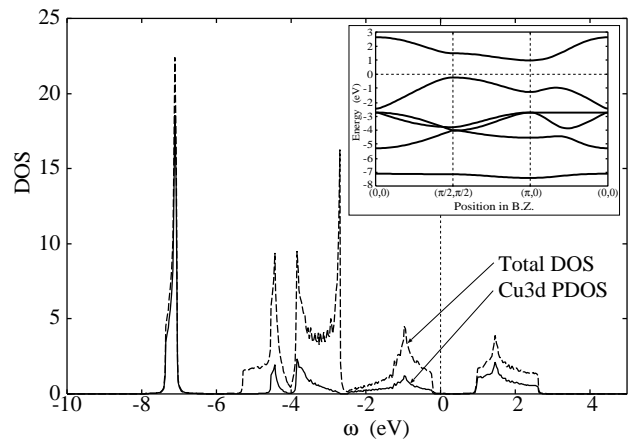


FIG. 4: The total density of states and the Cu3d<sub>x<sup>2</sup>-y<sup>2</sup></sub> partial density of states are shown by the solid and broken lines, respectively. The inset shows the band dispersion of the model in HF theory.

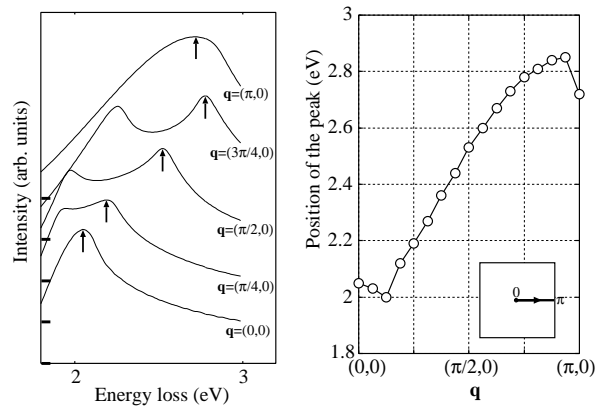


FIG. 5: Left panel shows details of the spectra along the line  $(0,0)$ - $(\pi,0)$  between  $\omega = 2$ -3 eV. The data are offset vertically, and the thick horizontal bars drawn on the left vertical axis denote the baseline for each spectrum. The arrows denote the positions of the main peak. Right panel shows the position of the main peak as a function of  $q$ .

fied somewhat by the RPA corrections. The correlation effects between Cu3d electrons cause an anisotropy and modify the simple  $s$ -wave scattering amplitude, and result in the enhancement and suppression of the spectral weight at  $q = (0,0)$  and  $q = (\pi,\pi)$ , respectively.

We focus our attention on the dispersive behavior of the low-energy peak at 2 eV. We display the detailed behaviors of the 2 eV peak in Fig. 5, along the line  $(0,0)$ - $(\pi,0)$ . We find that there is a fine structure in the 2 eV peak: the peak splits into two peaks. Such a fine structure is not observed in the experiment<sup>5</sup>, maybe due to the low resolution. The shift of the peak between the points  $(0,0)$  and  $(\pi,0)$  is about 0.8 eV. This is slightly smaller than the experimental result. We consider that this deviation originates from our underestimation of the O2p bandwidth.

#### IV. DISCUSSION

We have used the LDA parameters for the model. Although there are still much room for discussing the validity of the application of the LDA parameters to excitation processes, the parameters would provide a good starting point. To be more quantitative, the renormalization effects due to correlations should be taken into account in the future.

We briefly note some effects of other factors which are not included in the above calculations: effects of on-site Coulomb interaction  $U_{pp}$  between O2p electrons, inter-site Coulomb interaction  $U_{dp}$  between O2p and Cu3d electrons, higher orders in the core hole potential  $V$ , self-energy corrections and Coulomb interaction  $U_{3d-4p}$  between Cu3d and 4p electrons, multi-pair creation, phonons. We expect that these effects are not crucial in explaining the observed spectral properties.

We employed multiband RPA including  $U_{pp}$ , but found that  $U_{pp}$  only reinforces the effect of the Coulomb interaction  $U_{dd}$ . We cannot exclude the possibility that  $U_{dp}$  modifies the analytic properties of the spectral functions, i.e., novel poles of the spectral function could appear on the complex  $\omega$  plane near the real axis. In such a case, some peak structures related to a bound exciton mode would be added to the spectra. However, note that there is no necessity for the additional peak to be located around the observed positions at 2 and 4 eV. Such a novel structure would not be consistent with the experiment.

We could investigate the effects of higher orders of  $V$  by summing up the perturbation terms to the infinite order, similarly to  $T$ -matrix approximation for single impurity problems. We speculate from our preliminary work that the higher orders in  $V$  only negligibly modify the spectral shape, although they modify the absolute intensity of the spectra.

Concerning the self-energy corrections, detailed investigations are a future work. In x-ray absorption process,  $U_{3d-4p}$  could play an important role for ‘‘Extrinsic losses’’ (e.g., Ref. 11) through self-energy corrections, leaving

electron-hole pairs on the 3d band in the final state. But,  $U_{3d-4p}$  would not be so essential in the present RIXS process, since the 4p electron is annihilated rapidly with Cu1s hole in the final state of the RIXS.

Multi-pair creation processes may become more important for metals, leading to the Fermi edge singularity in the spectra. However multi-pair creation processes are not so essential in insulators, since they require much excitation energy (the energy per one pair is given by the insulating gap, about 2eV in the present case).

Regarding phonon effect, phonons can be excited in order to screen the core hole potential in the intermediate state. However, in the present RIXS, the phonon process cannot be the dominant process to screen the core hole potential, since the annihilation of the core hole is much faster than the screening process by phonons.

#### V. CONCLUSION

In conclusion, we note the following points. (i) We have not employed the physical picture that a kind of bound exciton formed by Coulomb interaction appears and moves in the CuO<sub>2</sub> plane. The two-peak structure of the observed spectra is attributable to the structure of the Cu3d partial density of states mixed with the O2p band, rather than some kind of bound exciton mode. (ii) The present formulation by the perturbative method is applicable to more complex and realistic electronic structures, in contrast to small cluster calculations and exact diagonalization techniques, whose applicability is limited to simple solids consisting of a few kinds of elements.

#### Acknowledgments

The authors are grateful to Dr. Y.J. Kim for the discussions. The numerical computations were partly performed at the Yukawa Institute Computer Facility in Kyoto University.

---

\* Electronic address: nomurat@spring8.or.jp

<sup>1</sup> A. Kotani and S. Shin, Rev. Mod. Phys. **73**, 203 (2001).

<sup>2</sup> C.-C. Kao, W. Caliebe, J. Hastings, and J.-M. Gillet, Phys. Rev. B **54**, 16361 (1996).

<sup>3</sup> J. Hill, C.-C. Kao, W. Caliebe, M. Matsubara, A. Kotani, J. Peng, and R. Greene, Phys. Rev. Lett. **80**, 4967 (1998).

<sup>4</sup> M. Hasan, E. Isaacs, Z.-X. Shen, L.L.Miller, K. Tsutsui, T. Tohyama, and S. Maekawa, Science **288**, 1811 (2000).

<sup>5</sup> Y. Kim, J. Hill, C. Burns, S. Wakimoto, R. Birgeneau, D. Casa, T. Cog, and C. Venkataraman, Phys. Rev. Lett. **89**, 177003 (2002).

<sup>6</sup> T. Inami, T. Fukuda, J. Mizuki, S. Ishihara, H. Kondo,

H. Nakao, T. Matsumura, K. Hirota, Y. Murakami, S. Maekawa, et al., Phys. Rev. B **67**, 045108 (2003).

<sup>7</sup> P. Platzman and E. Isaacs, Phys. Rev. B **57**, 11107 (1998).

<sup>8</sup> P. Nozières and E. Abrahams, Phys. Rev. B **10**, 3099 (1974).

<sup>9</sup> K. Tsutsui, T. Tohyama, and S. Maekawa, Phys. Rev. Lett. **83**, 3705 (1999).

<sup>10</sup> M. S. Hybertsen and M. Schluter, Phys. Rev. B **39**, 9028 (1989).

<sup>11</sup> J. Rehr, Found. Phys. **33**, 1735 (2003).